Supplementary Information

Marine natural products as leads against SARS-CoV-2 infection

Bhuwan Khatri Chhetri,[†,a] Philip R. Tedbury,[∇,a] Anne Marie Sweeney-Jones,[†] Luke Mani,[ξ] Katy Soapi,[ξ] Candela Manfredi,[¶] Eric Sorscher,[¶] Stefan G. Sarafianos,[∇] and Julia Kubanek[*,†,‡,§,Θ]

[†] School of Chemistry and Biochemistry, Georgia Institute of Technology, Atlanta, GA 30332, USA

[‡] Center for Microbial Dynamics and Infection, Georgia Institute of Technology, Atlanta, GA 30332, USA

[§] School of Biological Sciences, Georgia Institute of Technology, Atlanta, GA 30332, USA

[∇] Laboratory of Biochemical Pharmacology, Department of Pediatrics, Emory University School of Medicine, Atlanta, GA 30322, USA

[ξ] Institute of Applied Sciences, University of South Pacific, Suva, Fiji

[¶] Department of Pediatrics, Division of Pulmonary Medicine, Emory University School of Medicine, Atlanta, Georgia, USA.

[Θ] Parker H. Petit Institute for Bioengineering and Bioscience, Georgia Institute of Technology, Atlanta, GA 30332, USA

[a] These authors contributed equally
[*] Author to whom correspondence should be addressed.

Content

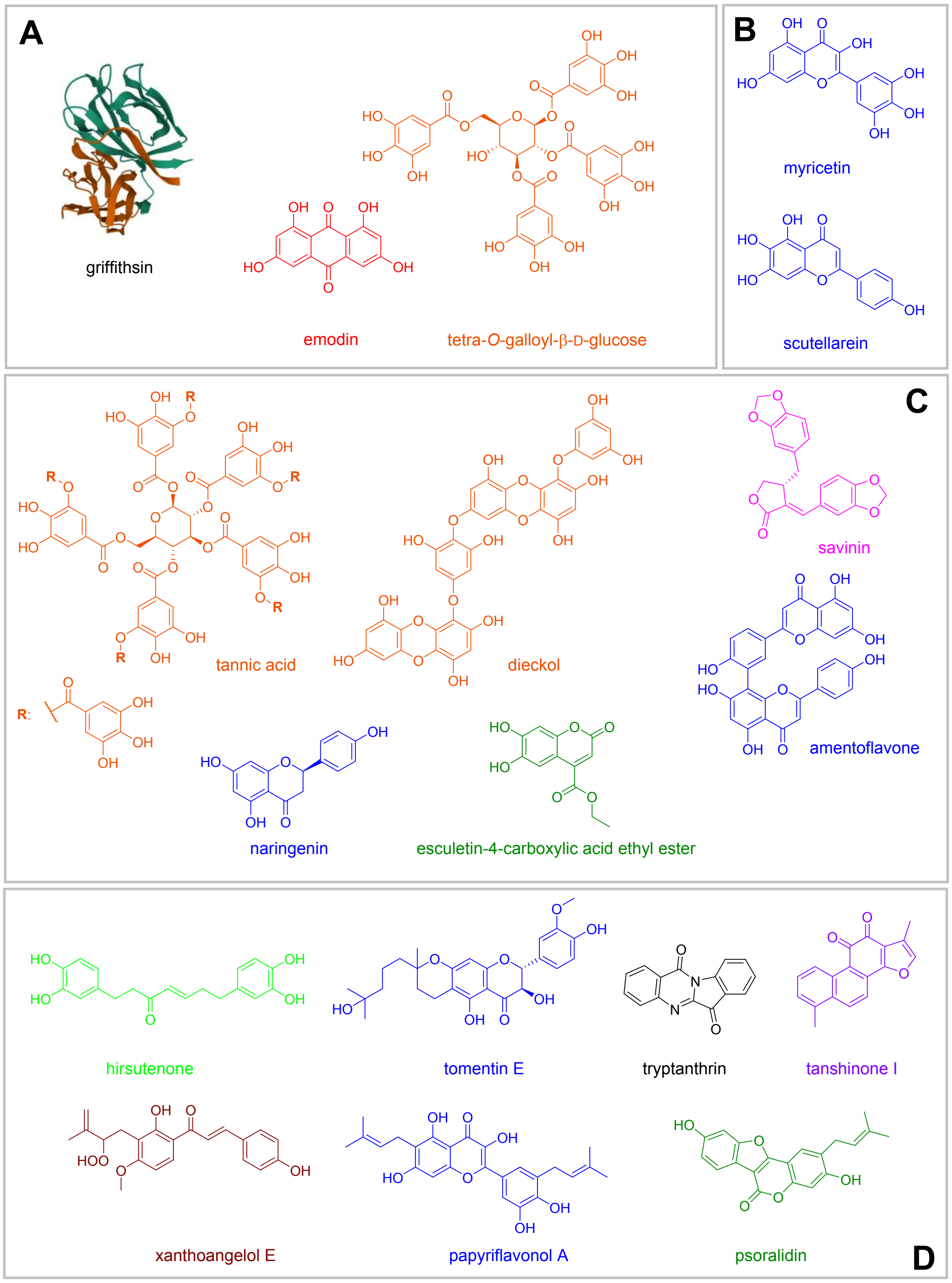

Figure S1. Natural products with promising literature-reported activity against the coronavirus SARS-CoV, which causes SARS. These natural products are categorized by their putative molecular targets: **A**. spike protein of SARS-CoV.[1-3] The structure of griffithsin as reported in the Protein Data Bank (PDB): 2GTY at www.rcsb.org was generated using Mol* Viewer,[4] **B**. viral helicase,[5] **C**. SARS-CoV chymotrypsin-like protease ($3CL^{pro}$)/ main protease (M^{pro}),[6-11] and **D**. papain-like cysteine protease (PL^{pro}).[12-18] Structural classes of natural products are depicted by color: anthraquinone (red), tannins (orange), flavonoids (blue), alkaloid (black), terpene (purple), lignan (pink), coumarins (dark green), diarylheptanoid (light green), and chalcone (brown).

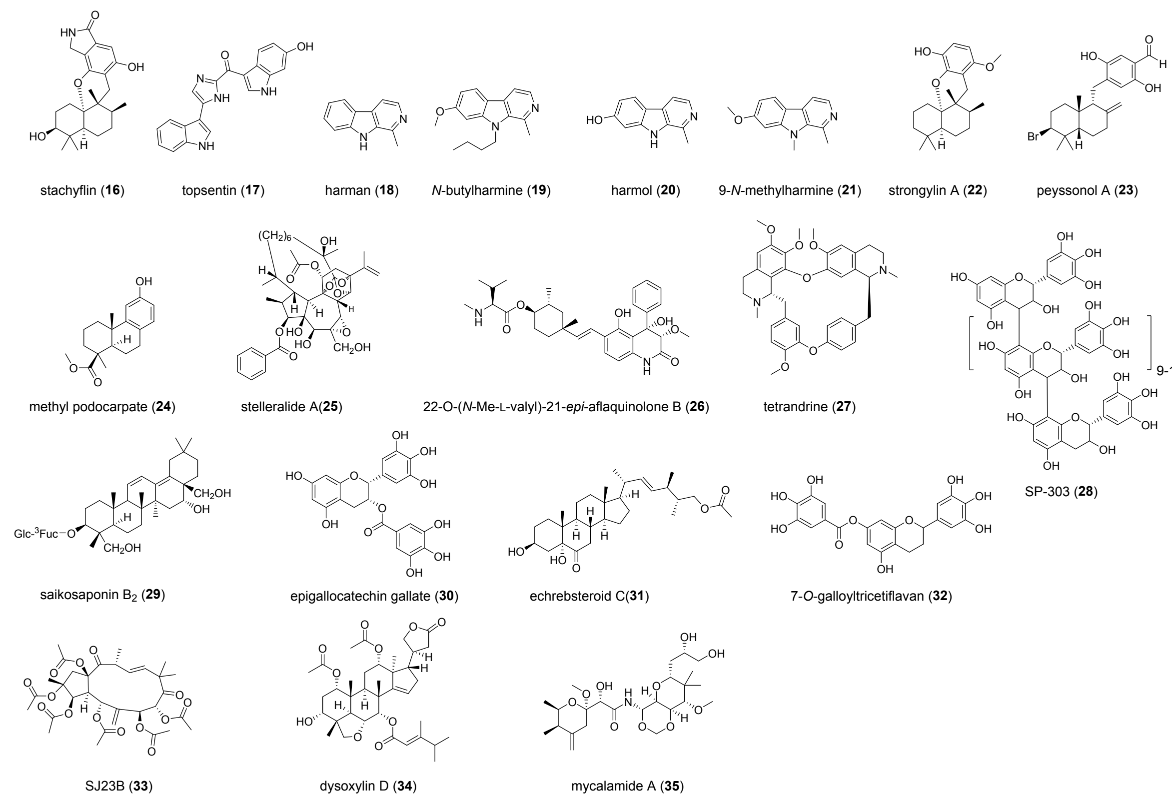

Figure S2. Additional natural products with literature-reported antiviral activity. Stachyflin (**16**): active against influenza A virus,[19-21] topsentin (**17**): active against coronavirus A59,[22] harman (**18**), *N*-butyl harmine (**19**): inhibit HIV viral replication,[23] harmol (**20**), 9-*N*-methylharmine (**21**): active against dengue virus,[24] strongylin A (**22**): active against influenza strain PR-8,[25] peyssonol A (**23**): shows anti-HIV-1 activity,[26, 27] methyl podocarpate (**24**): active against influenza A virus,[28] stelleralide A (**25**): potent anti-HIV activity,[29] 22-O-(*N*-Me-L-valyl)-21-*epi*-aflaquinolone B (**26**): potent anti-Respiratory Syncytial Virus (RSV) activity,[30] tetrandrine (**27**): active against human coronavirus OC43,[31] SP-303 (**28**): active against of DNA and RNA viruses including respiratory syncytial virus, influenzas A virus and parainfluenza virus,[32] saikosaponin B_2 (**29**): active against human coronavirus 229E,[33] epigallocatechin gallate (**30**): active against SARS-CoV-2 strain,[34] echrebsteroid C (**31**): active against RSV,[35] 7-*O*-galloyltricetiflavan (**32**): active against RSV,[36] SJ23B (**33**): potent activity against HIV,[37] dysoxylin D (**34**): potent anti-RSV activity,[38] mycalamide (**35**): active against coronavirus A59.[39]

Figure S3. Collection photo for *Fascaplysinopsis reticulata*.

Characterization data for Homofascaplysin A (1): ^{1}H NMR (800 MHz, CD_3OD): δ_H 9.32 (1H, d, *J* = 6.5 Hz, H-6), 8.82 (1H, d, *J* = 6.5 Hz, H-7), 8.47 (1H, d, *J* = 8.0 Hz, H-8), 8.26 (1H, d, *J* = 8.0 Hz, H-4), 7.90 (1H, d, *J* = 7.4 Hz, H-1), 7.84 (2H, m, H-10, H-11), 7.74 (1H, t, *J* = 7.5, H-3), 7.68 (1H, t, *J* = 7.5 Hz, H-2), 7.51 (1H, ddd, *J* = 1.2, 7.2, 8.3 Hz, H-9), 4.27 (1H, d, *J* = 18.6 Hz, H-14), 4.18 (1H, d, *J* = 18.6 Hz, H-14), 1.98 (3H, s, H-16); ^{13}C NMR (201 MHz, CD_3OD): δ_C 206.5 (C-15), 146.8 (C-11a), 144.9 (C-12b), 142.6 (C-4a), 138.6 (C-1a), 136.6 (C-7a), 134.0 (C-10), 132.2 (C-3), 132.1 (C-12a), 131.9 (C-2), 125.8 (C-1), 124.4 (C-6), 124.4 (C-8), 123.7 (C-9), 121.4 (C-7b), 118.4 (C-7), 115.2 (C-4), 114.1 (C-11), 79.2 (C-13), 51.5 (C-14), 30.1 (C-16); HRMS (ESI) *m/z* $[M]^+$ calculated for $C_{21}H_{17}N_2O_2^+$, 329.1285; found, 329.1288. Note: 2D NMR spectroscopic data (COSY, HSQC, HMBC) including 1D selective TOCSY, NOESY (not shown) were acquired for ^{1}H and ^{13}C chemical shift annotation. The ^{13}C NMR chemical shift for C12a in **3** has been reported to be 122.3 ppm in literature.[40] However, we found C12a to be 132.1 ppm which aligns with the ^{13}C NMR shift of 132.4 ppm as reported for a close structural analog 3-bromofascaplysin A.[41] Furthermore, it was also confirmed that the discrepancy in ^{13}C NMR chemical shift of C12a was not an effect of counter ion (in the literature,[40] **1** was isolated using a gradient elution of 45:55 to 100:0 MeOH/H_2O with 0.05% TFA, and hence the counter ion in the purified molecule was CF_3COO^-) by acquiring ^{13}C NMR spectroscopic data for MeOH:H_2O (0.05% TFA) treated **1**. Note: For bioassays, **1** with CF_3COO^- as counter ion was used. The absolute configuration of **1** was assigned as 13*S* by considering a previous report on its isolation from *Fascaplysinopsis reticulata* (the same species from which we isolated **1**).[42] The authors reported a specific optical rotation of −9.36°, consistent with a another study that determined its absolute configuration as 13*S* by comparison of the experimental ECD spectrum with a DFT-based simulated spectrum.[41]

Characterization data for (+)**-aureol** (**2**): $[\alpha]^{23}_{D}$ +47 (*c* 0.3, $CHCl_3$); ^{1}H NMR (800 MHz, $CDCl_3$): δ_H 6.59 (1H, d, J = 8.5 Hz, H-18), 6.57 (1H, dd, J = 8.7, 2.7 Hz, H-19), 6.49 (1H, d, J = 2.5 Hz, H-21), 3.36 (1H, d, J = 17.0 Hz, H-15a), 2.07 (1H, m, H-2a), 2.02 (1H, m, H-7a), 1.95 (1H, d, J = 17.0 Hz, H-15b), 1.81 (1H, m, H-1a), 1.76 (1H, m, H-1b), 1.67 (1H, m, H-6a), 1.65 (1H, m, H-8), 1.55 (1H, m, H-6b), 1.46 (1H, m, H-2b), 1.44 (1H, m, H-5), 1.41 (1H, m, H-3a), 1.34 (1H, m, H-7b), 1.18 (1H, m, H-3b), 1.10 (3H, d, 7.5 Hz, H-13), 1.06 (3H, s, H-12), 0.91 (3H, s, H-14), 0.77 (3H, s, H-11); ^{13}C NMR (201 MHz, $CDCl_3$): δ_C 148.9 (C-20), 145.6 (C-17), 122.2 (C-16), 117.3 (C-18), 115.2 (C-19), 114.2 (C-21), 82.4 (C-10), 44.0 (C-5), 39.4 (C-8), 38.2 (C-9), 37.5 (C-15), 34.0 (C-4), 34.0 (C-3), 32.1 (C-12), 30.0 (C-11), 29.4 (C-7), 28.0 (C-1), 22.3 (C-6), 20.3 (C-14), 18.5 (C-2), 17.5 (C-13); HRMS (ESI) *m/z* $[M + H]^+$ calculated for $C_{21}H_{31}O_2^+$, 315.2319; found, 315.2319. The identity of **2** was confirmed by comparison of ^{1}H,^{13}C NMR spectroscopic data and specific optical rotation with literature.[43, 44] Additionally, 2D NMR spectroscopic data (COSY, HSQC, HMBC) including 1D selective TOCSY, NOESY (not shown) were acquired for ^{1}H and ^{13}C chemical shift annotation (**Figure S8**).

Characterization data for Haliclonacyclamine A (**11**): ^{1}H NMR (800 MHz, $CDCl_3$): δ_H 13.07 (bs, 2H), 5.33 (m, 2H), 5.26 (m, 2H), 3.31 (d, J = 6.5 Hz, 1H), 3.24 – 3.03 (m, 8H), 2.84 (t, J = 12.7 Hz, 1H), 2.61 (m, 1H), 2.36 (m, 2H), 2.26 – 2.18 (m, 5H), 2.13 – 2.01 (m, 7H), 1.95 (d, J = 15.3 Hz, 1H), 1.89 (m, 1H), 1.66 – 1.09 (m, 24H), 0.97 (m, 1H); ^{13}C NMR (200 MHz, $CDCl_3$): δ_C 132.2, 131.8, 129.9, 129.1, 57.0, 56.2, 56.1, 55.0, 50.8, 45.7, 40.3, 38.2, 34.9, 34.9, 32.7, 32.6, 31.6, 31.5, 29.3, 29.2, 29.1, 28.8, 27.6, 27.5, 26.8, 26.4, 26.4, 26.3, 26.3, 26.1, 20.8, 20.7; HRMS (ESI) *m/z* $[M+H]^+$ calculated for $C_{32}H_{57}N_2^+$, 469.4517; found low-resolution MS (ESI) 469.2.

X-ray crystallographic analysis of haliclonacyclamine A (**11**): About 5 mg of **11** was dissolved in 1 ml of hexanes:ethylacetate (1:3). Slow evaporation of the solvent at room temperature (over three days) led to the formation of colorless prism-shaped crystals of **11**. A suitable crystal 0.33×0.25×0.12 mm^3 was selected and mounted on a loop with paratone oil on an XtaLAB Synergy, Dualflex, HyPix diffractometer. The crystal was kept at a steady T = 100(1) K during data collection. The structure was solved with the ShelXT structure solution program using the Intrinsic Phasing solution method and by using Olex2 as the graphical interface.[45, 46] The model was refined with version 2018/3 of ShelXL using Least Squares minimization.[47] Crystal data: $C_{36}H_{60}F_6N_2O_5$, M_r = 714.86, monoclinic, $P2_1$ (No. 4), a = 10.9305(2) Å, b = 9.4445(2) Å, c = 18.5476(5) Å, β = 93.264(2)°, $\alpha = \gamma$ = 90°, V = 1911.61(8) Å^3, T = 100.00(10) K, Z = 1, Z' = 0.5, $\mu(MoK_\alpha)$ = 0.101, 37746 reflections measured, 16246 unique (R_{int} = 0.0282) which were used in all calculations. The final wR_2 was 0.2698 (all data) and R_1 was 0.0875 (I > 2σ(I)) (**Figure S11**).[48]

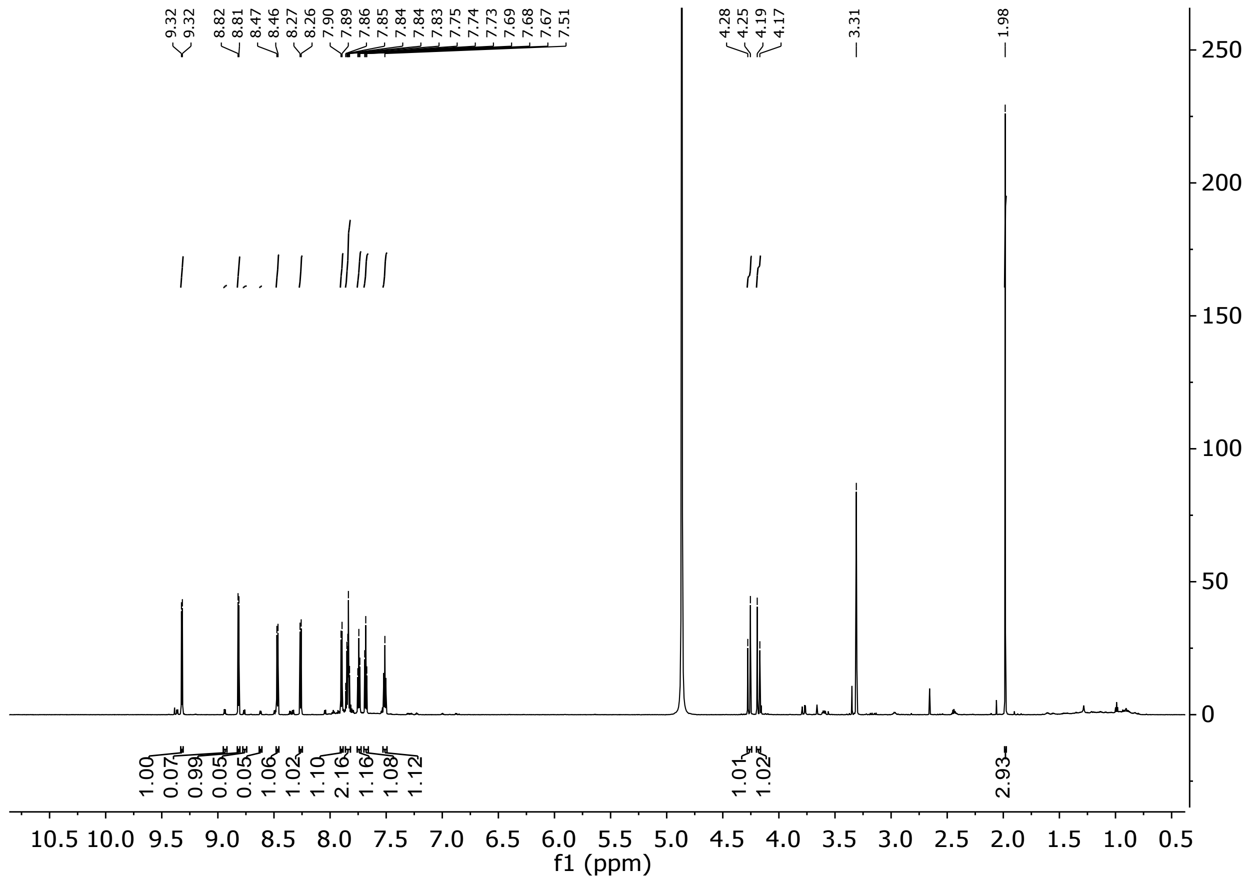

Figure S4. [1]H NMR spectrum for homofascaplysin A (**1**) in CD_3OD (800 MHz)

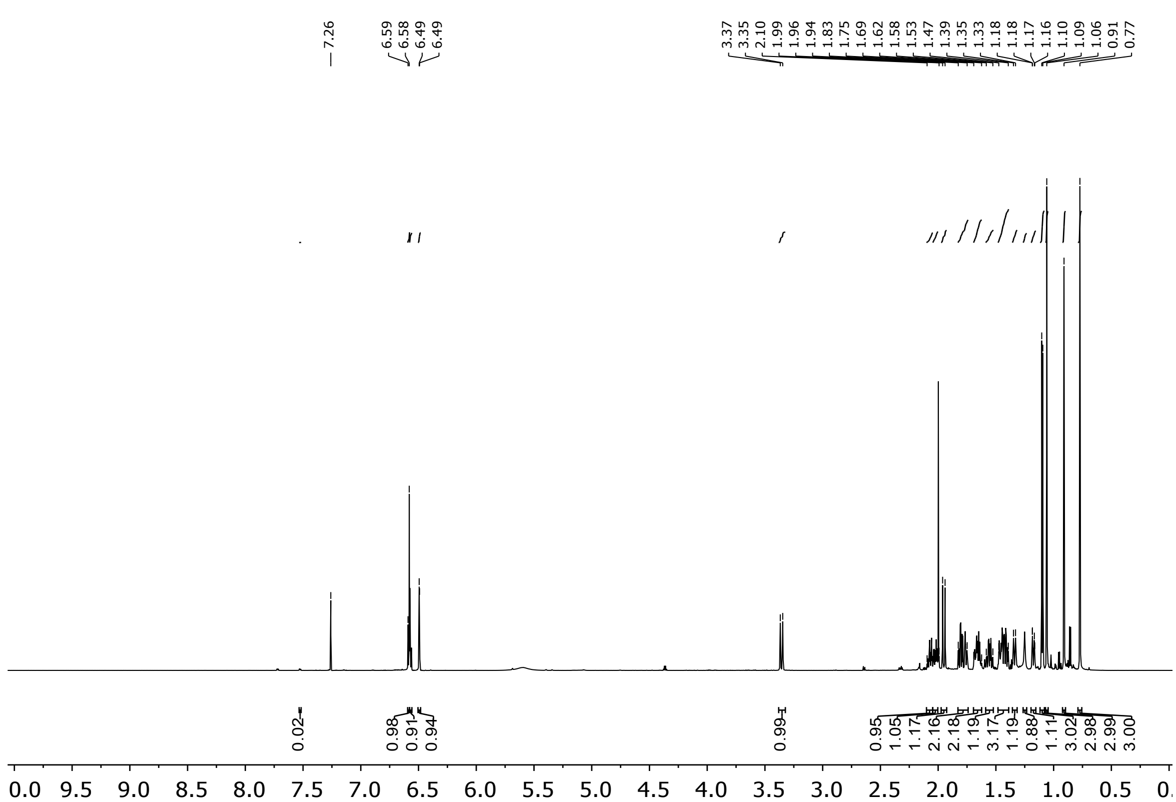

Figure S5. [1]H NMR spectrum for (+)-aureol (**2**) in $CDCl_3$ (800 MHz)

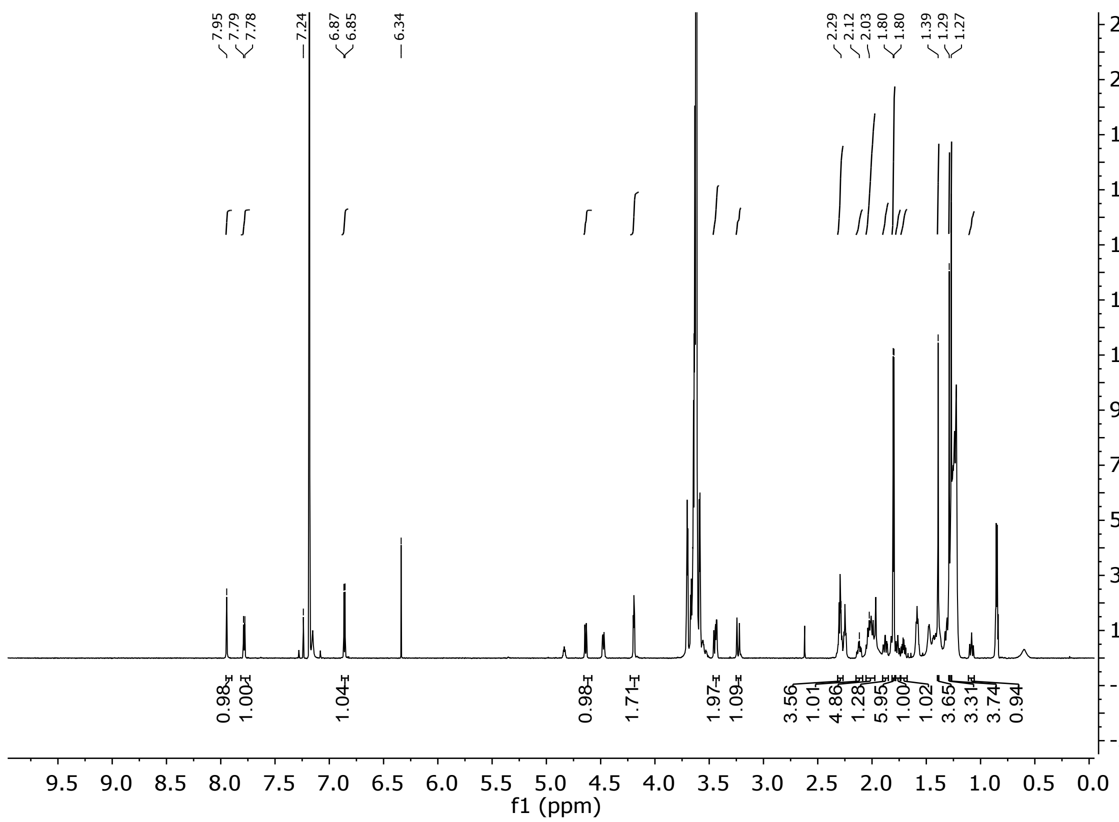

Figure S6. ^{1}H NMR spectrum for bromophycolide A (**3**) in $CDCl_3$ (800 MHz)

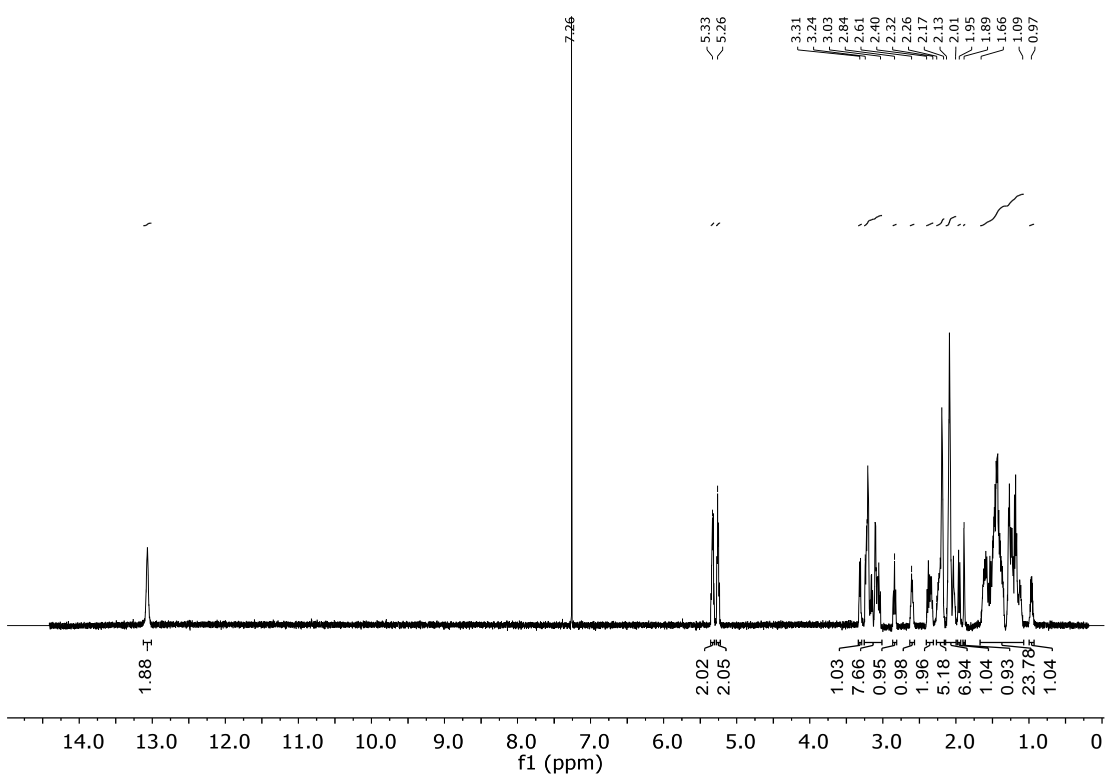

Figure S7. ^{1}H NMR spectrum for haliclonacyclamine A (**11**) in $CDCl_3$ (800 MHz)

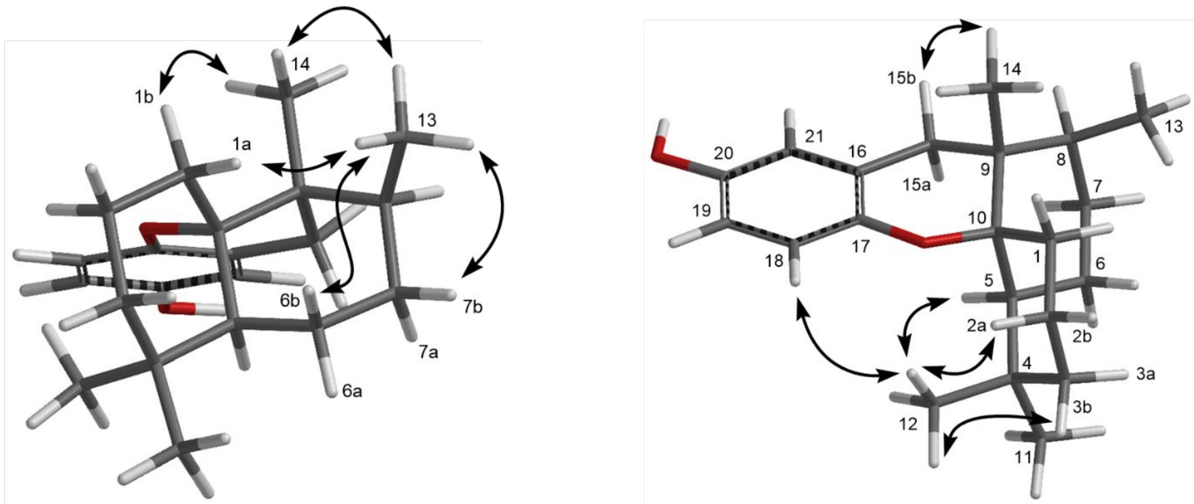

Figure S8. Key NOESY correlations used to confirm the relative configuration and annotate methylene protons present in (+)-aureol (**2**).

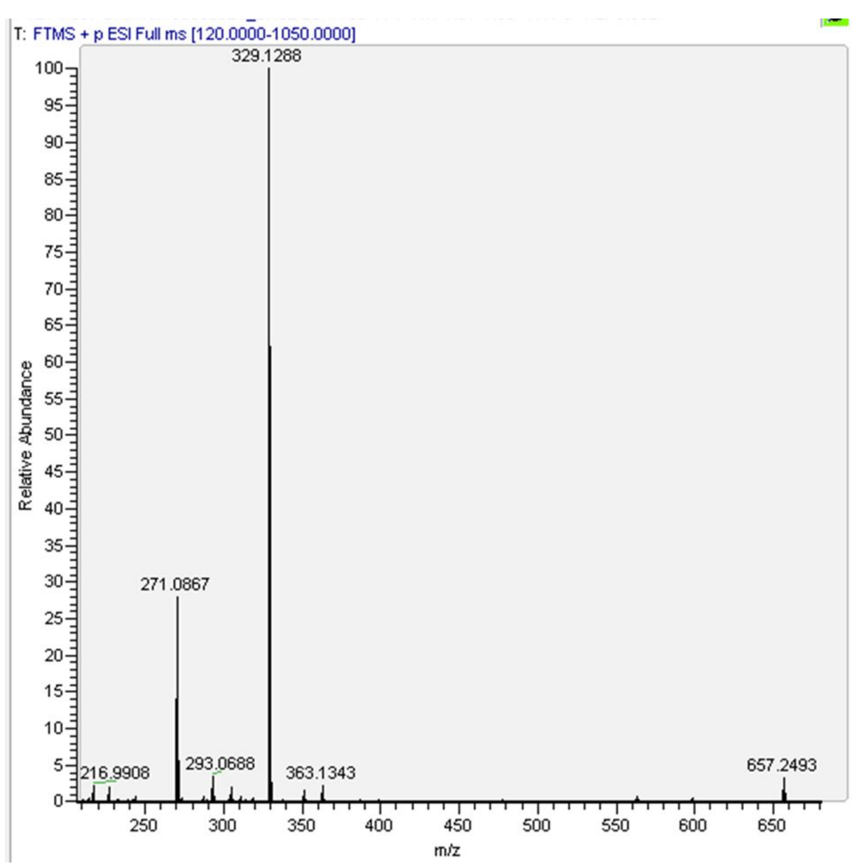

Figure S9. Positive ionization mode HRMS data for homofascaplysin A (**1**)

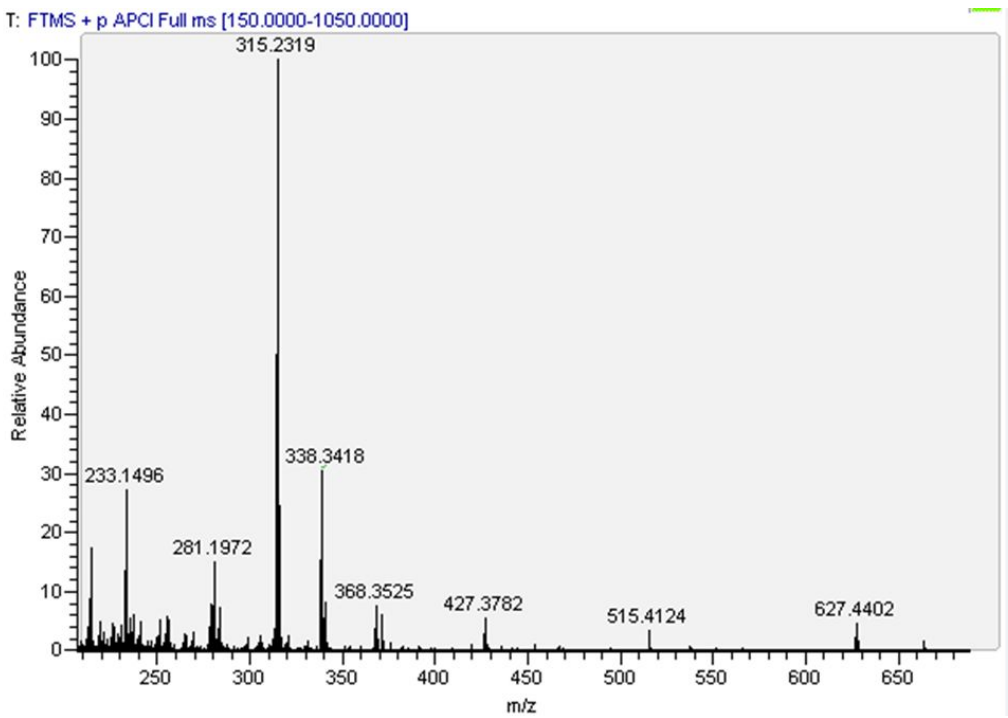

Figure S10. Positive ionization mode HRMS data for (+)-aureol (**2**)

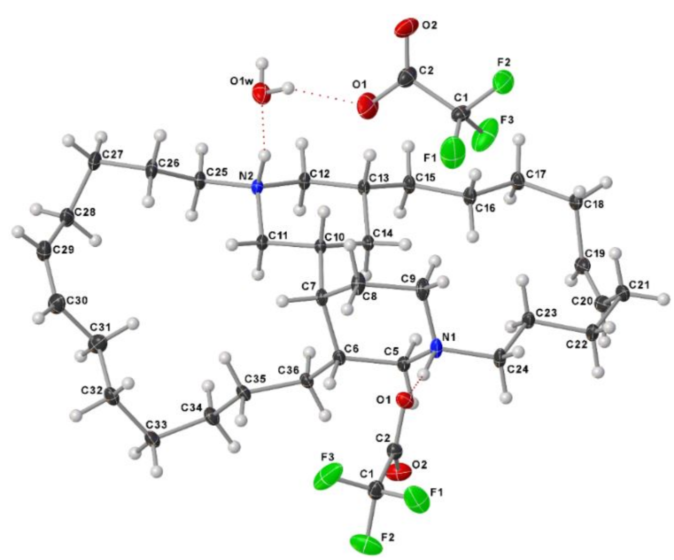

Figure S11. X-ray crystallographic structure for haliclonacyclamine A (**11**)

References

1. Ho, T. Y.; Wu, S. L.; Chen, J. C.; Li, C. C.; Hsiang, C. Y. Emodin blocks the SARS coronavirus spike protein and angiotensin-converting enzyme 2 interaction. *Antivir. Res.* **2007**, *74* (2), 92-101.
2. Yi, L.; Li, Z.; Yuan, K.; Qu, X.; Chen, J.; Wang, G.; Zhang, H.; Luo, H.; Zhu, L.; Jiang, P.; Chen, L.; Shen, Y.; Luo, M.; Zuo, G.; Hu, J.; Duan, D.; Nie, Y.; Shi, X.; Wang, W.; Han, Y.; Li, T.; Liu, Y.; Ding, M.; Deng, H.; Xu, X. Small Molecules Blocking the Entry of Severe Acute Respiratory Syndrome Coronavirus into Host Cells. *J. Virol.* **2004**, *78* (20), 11334-11339.
3. O'Keefe, B. R.; Giomarelli, B.; Barnard, D. L.; Shenoy, S. R.; Chan, P. K.; McMahon, J. B.; Palmer, K. E.; Barnett, B. W.; Meyerholz, D. K.; Wohlford-Lenane, C. L.; McCray, P. B., Jr. Broad-Spectrum *In Vitro* Activity and *In Vivo* Efficacy of the Antiviral Protein Griffithsin against Emerging Viruses of the Family *Coronaviridae*. *J. Virol.* **2010**, *84* (5), 2511-2521.
4. Sehnal, D.; Bittrich, S.; Deshpande, M.; Svobodová, R.; Berka, K.; Bazgier, V.; Velankar, S.; Burley, S. K.; Koča, J.; Rose, A. S. Mol* Viewer: modern web app for 3D visualization and analysis of large biomolecular structures. *Nucleic Acids Res.* **2021**, *49* (W1), W431-W437.
5. Yu, M. S.; Lee, J.; Lee, J. M.; Kim, Y.; Chin, Y. W.; Jee, J. G.; Keum, Y. S.; Jeong, Y. J. Identification of myricetin and scutellarein as novel chemical inhibitors of the SARS coronavirus helicase, nsP13. *Bioorg. Med. Chem. Lett.* **2012**, *22* (12), 4049-4054.
6. Abdallah, H. M.; El-Halawany, A. M.; Sirwi, A.; El-Araby, A. M.; Mohamed, G. A.; Ibrahim, S. R. M.; Koshak, A. E.; Asfour, H. Z.; Awan, Z. A.; M, A. E. Repurposing of Some Natural Product Isolates as SARS-COV-2 Main Protease Inhibitors via In Vitro Cell Free and Cell-Based Antiviral Assessments and Molecular Modeling Approaches. *Pharmaceuticals* **2021**, *14* (3), 213.
7. Wang, S. C.; Chen, Y.; Wang, Y. C.; Wang, W. J.; Yang, C. S.; Tsai, C. L.; Hou, M. H.; Chen, H. F.; Shen, Y. C.; Hung, M. C. Tannic acid suppresses SARS-CoV-2 as a dual inhibitor of the viral main protease and the cellular TMPRSS2 protease. *Am. J. Cancer Res.* **2020**, *10* (12), 4538-4546.
8. Wen, C. C.; Kuo, Y. H.; Jan, J. T.; Liang, P. H.; Wang, S. Y.; Liu, H. G.; Lee, C. K.; Chang, S. T.; Kuo, C. J.; Lee, S. S.; Hou, C. C.; Hsiao, P. W.; Chien, S. C.; Shyur, L. F.; Yang, N. S. Specific Plant Terpenoids and Lignoids Possess Potent Antiviral Activities against Severe Acute Respiratory Syndrome Coronavirus. *J. Med. Chem.* **2007**, *50* (17), 4087-4095.
9. Park, J. Y.; Kim, J. H.; Kwon, J. M.; Kwon, H. J.; Jeong, H. J.; Kim, Y. M.; Kim, D.; Lee, W. S.; Ryu, Y. B. Dieckol, a SARS-CoV 3CL^{pro} inhibitor, isolated from the edible brown algae *Ecklonia cava*. *Bioorg. Med. Chem.* **2013**, *21* (13), 3730-3737.
10. Lira, S. P. d.; Seleghim, M. H.; Williams, D. E.; Marion, F.; Hamill, P.; Jean, F.; Andersen, R. J.; Hajdu, E.; Berlinck, R. G. A SARS-Coronovirus 3CL Protease Inhibitor Isolated from the Marine Sponge *Axinella* cf. *corrugata*: Structure Elucidation and Synthesis. *J. Braz. Chem. Soc.* **2007**, *18* (2), 440-443.
11. Ryu, Y. B.; Jeong, H. J.; Kim, J. H.; Kim, Y. M.; Park, J. Y.; Kim, D.; Nguyen, T. T.; Park, S. J.; Chang, J. S.; Park, K. H.; Rho, M. C.; Lee, W. S. Biflavonoids from *Torreya nucifera* displaying SARS-CoV 3CL^{pro} inhibition. *Bioorg. Med. Chem. Lett.* **2010**, *18* (22), 7940-7947.
12. Tsai, Y. C.; Lee, C. L.; Yen, H. R.; Chang, Y. S.; Lin, Y. P.; Huang, S. H.; Lin, C. W. Antiviral Action of Tryptanthrin Isolated from *Strobilanthes cusia* Leaf against Human Coronavirus NL63. *Biomolecules* **2020**, *10* (3), 366.
13. Kim, D. W.; Seo, K. H.; Curtis-Long, M. J.; Oh, K. Y.; Oh, J. W.; Cho, J. K.; Lee, K. H.; Park, K. H. Phenolic phytochemical displaying SARS-CoV papain-like protease inhibition from the seeds of *Psoralea corylifolia*. *J. Enzyme Inhib. Med. Chem.* **2014**, *29* (1), 59-63.
14. Park, J. Y.; Jeong, H. J.; Kim, J. H.; Kim, Y. M.; Park, S. J.; Kim, D.; Park, K. H.; Lee, W. S.; Ryu, Y. B. Diarylheptanoids from *Alnus japonica* Inhibit Papain-Like Protease of Severe Acute Respiratory Syndrome Coronavirus. *Biol. Pharm. Bull.* **2012**, *35* (11), 2036-2042.
15. Cho, J. K.; Curtis-Long, M. J.; Lee, K. H.; Kim, D. W.; Ryu, H. W.; Yuk, H. J.; Park, K. H. Geranylated flavonoids displaying SARS-CoV papain-like protease inhibition from the fruits of *Paulownia tomentosa*. *Bioorg. Med. Chem.* **2013**, *21* (11), 3051-3057.
16. Park, J. Y.; Kim, J. H.; Kim, Y. M.; Jeong, H. J.; Kim, D. W.; Park, K. H.; Kwon, H. J.; Park, S. J.; Lee, W. S.; Ryu, Y. B. Tanshinones as selective and slow-binding inhibitors for SARS-CoV cysteine proteases. *Bioorg. Med. Chem.* **2012**, *20* (19), 5928-5935.

17. Park, J. Y.; Yuk, H. J.; Ryu, H. W.; Lim, S. H.; Kim, K. S.; Park, K. H.; Ryu, Y. B.; Lee, W. S. Evaluation of polyphenols from *Broussonetia papyrifera* as coronavirus protease inhibitors. *J. Enzyme Inhib. Med. Chem.* **2017**, *32* (1), 504-515.
18. Park, J. Y.; Ko, J. A.; Kim, D. W.; Kim, Y. M.; Kwon, H. J.; Jeong, H. J.; Kim, C. Y.; Park, K. H.; Lee, W. S.; Ryu, Y. B. Chalcones isolated from *Angelica keiskei* inhibit cysteine proteases of SARS-CoV. *J. Enzyme Inhib. Med. Chem.* **2016**, *31* (1), 23-30.
19. Minagawa, K.; Kouzuki, S.; Yoshimoto, J.; Kawamura, Y.; Tani, H.; Iwata, T.; Terui, Y.; Nakai, H.; Yagi, S.; Hattori, N.; Fujiwara, T.; Kamigauchi, T. Stachyflin and Acetylstachyflin, Novel Anti-influenza A Virus Substances, Produced by *Stachybotrys* sp. RF-7260. I. Isolation, Structure Elucidation and Biological Activities. *J. Antibiot.* **2002**, *55* (2), 155-164.
20. Minagawa, K.; Kouzuki, S.; Kamigauchi, T. Stachyflin and Acetylstachyflin, Novel Anti-influenza A Virus Substances, Produced by *Stachybotrys* sp. RF-7260. II. Synthesis and Preliminary Structure-Activity Relationships of Stachyflin Derivatives. *J. Antibiot.* **2002**, *55* (2), 165-171.
21. Yoshimoto, J.; Yagi, S.; Ono, J.; Sugita, K.; Hattori, N.; Fujioka, T.; Fujiwara, T.; Sugimoto, H.; Hashimoto, N. Development of Anti-influenza Drugs: II. Improvement of Oral and Intranasal Absorption and the Anti-influenza Activity of Stachyflin Derivatives. *J. Pharm. Pharmacol.* **2000**, *52* (10), 1247-1255.
22. Tsujii, S.; Rinehart, K. L.; Gunasekera, S. P.; Kashman, Y.; Cross, S. S.; Lui, M. S.; Pomponi, S. A.; Diaz, M. C. Topsentin, Bromotopsentin, and Dihydrodeoxybromotopsentin: Antiviral and Antitumor Bis (indolyl) imidazoles from Caribbean Deep-Sea Sponges of the Family Halichondriidae. Structural and Synthetic Studies. *J. Org. Chem.* **1988**, *53* (23), 5446-5453.
23. Ishida, J.; Wang, H. K.; Oyama, M.; Cosentino, M. L.; Hu, C. Q.; Lee, K. H. Anti-AIDS agents. 46.[1] Anti-HIV Activity of Harman, an Anti-HIV Principle from *Symplocos setchuensis*, and Its Derivatives. *J. Nat. Prod.* **2001**, *64* (7), 958-960.
24. Quintana, V. M.; Piccini, L. E.; Panozzo Zénere, J. D.; Damonte, E. B.; Ponce, M. A.; Castilla, V. Antiviral activity of natural and synthetic β-carbolines against dengue virus. *Antivir. Res.* **2016**, *134*, 26-33.
25. Wright, A. E.; Rueth, S. A.; Cross, S. S. An Antiviral Sesquiterpene Hydroquinone from the Marine Sponge *Strongylophora hartmani*. *J. Nat. Prod.* **1991**, *54* (4), 1108-1111.
26. Loya, S.; Bakhanashvili, M.; Kashman, Y.; Hizi, A. Peyssonols A and B, Two Novel Inhibitors of the Reverse Transcriptases of Human Immunodeficiency Virus Types 1 and 2. *Arch. Biochem. Biophys.* **1995**, *316* (2), 789-796.
27. Treitler, D. S.; Li, Z.; Krystal, M.; Meanwell, N. A.; Snyder, S. A. Evaluation of HIV-1 inhibition by stereoisomers and analogues of the sesquiterpenoid hydroquinone peyssonol A. *Bioorg. Med. Chem. Lett.* **2013**, *23* (7), 2192-2196.
28. Dang, Z.; Jung, K.; Zhu, L.; Xie, H.; Lee, K. H.; Chen, C. H.; Huang, L. Phenolic Diterpenoid Derivatives as Anti-Influenza a Virus Agents. *ACS Med. Chem. Lett.* **2015**, *6* (3), 355-358.
29. Asada, Y.; Sukemori, A.; Watanabe, T.; Malla, K. J.; Yoshikawa, T.; Li, W.; Koike, K.; Chen, C. H.; Akiyama, T.; Qian, K.; Nakagawa-Goto, K.; Morris-Natschke, S. L.; Lee, K. H. Stelleralides A-C, Novel Potent Anti-HIV Daphnane-Type Diterpenoids from *Stellera chamaejasme* L. *Org. Lett.* **2011**, *13* (11), 2904-2907.
30. Chen, M.; Shao, C. L.; Meng, H.; She, Z. G.; Wang, C. Y. Anti-Respiratory Syncytial Virus Prenylated Dihydroquinolone Derivatives from the Gorgonian-Derived fungus *Aspergillus* sp. XS-20090B15. *J. Nat. Prod.* **2014**, *77* (12), 2720-2724.
31. Kim, D. E.; Min, J. S.; Jang, M. S.; Lee, J. Y.; Shin, Y. S.; Song, J. H.; Kim, H. R.; Kim, S.; Jin, Y. H.; Kwon, S. Natural Bis-Benzylisoquinoline Alkaloids-Tetrandrine, Fangchinoline, and Cepharanthine, Inhibit Human Coronavirus OC43 Infection of MRC-5 Human Lung Cells. *Biomolecules* **2019**, *9* (11), 696.
32. Ubillas, R.; Jolad, S. D.; Bruening, R. C.; Kernan, M. R.; King, S. R.; Sesin, D. F.; Barrett, M.; Stoddart, C. A.; Flaster, T.; Kuo, J.; Ayala, F.; Meza, E.; Castañel, M.; McMeekin, D.; Rozhon, E.; Tempesta, M. S.; Barnard, D.; Huffman, J.; Smee, D.; Sidwell, R.; Soike, K.; Brazier, A.; Safrin, S.; Orlando, R.; Kenny, P. T.; Berova, N.; Nakanishi, K. SP-303, an Antiviral Oligomeric Proanthocyanidin from the Latex of *Croton lechleri* (Sangre de Drago). *Phytomedicine* **1994**, *1* (2), 77-106.
33. Cheng, P. W.; Ng, L. T.; Chiang, L. C.; Lin, C. C. Antiviral Effects of Saikosaponins on Human Coronavirus 229E *in vitro*. *Clin. Exp. Pharmacol. Physiol.* **2006**, *33* (7), 612-616.

34. Hong, S.; Seo, S. H.; Woo, S. J.; Kwon, Y.; Song, M.; Ha, N. C. Epigallocatechin Gallate Inhibits the Uridylate-Specific Endoribonuclease Nsp15 and Efficiently Neutralizes the SARS-CoV-2 Strain. *J. Agric. Food Chem.* **2021**, *69* (21), 5948-5954.
35. Cao, F.; Shao, C. L.; Chen, M.; Zhang, M. Q.; Xu, K. X.; Meng, H.; Wang, C. Y. Antiviral C-25 Epimers of 26-Acetoxy Steroids from the South China Sea Gorgonian *Echinogorgia rebekka*. *J. Nat. Prod.* **2014**, *77* (6), 1488-1493.
36. Li, Y.; Leung, K. T.; Yao, F.; Ooi, L. S.; Ooi, V. E. Antiviral Flavans from the Leaves of *Pithecellobium clypearia*. *J. Nat. Prod.* **2006**, *69* (5), 833-835.
37. Bedoya, L. M.; Márquez, N.; Martínez, N.; Gutiérrez-Eisman, S.; Alvarez, A.; Calzado, M. A.; Rojas, J. M.; Appendino, G.; Muñoz, E.; Alcamí, J. SJ23B, a jatrophane diterpene activates classical PKCs and displays strong activity against HIV *in vitro*. *Biochem. Pharmacol.* **2009**, *77* (6), 965-978.
38. Chen, J. L.; Kernan, M. R.; Jolad, S. D.; Stoddart, C. A.; Bogan, M.; Cooper, R. Dysoxylins A-D, Tetranortriterpenoids with Potent Anti-RSV Activity from *Dysoxylum gaudichaudianum*. *J. Nat. Prod.* **2007**, *70* (2), 312-315.
39. Perry, N. B.; Blunt, J. W.; Munro, M. H.; Pannell, L. K. Mycalamide A, an antiviral compound from a New Zealand sponge of the genus Mycale. *J. Am. Chem. Soc.* **1988**, *110* (14), 4850-4851.
40. Kirsch, G.; Köng, G. M.; Wright, A. D.; Kaminsky, R. A new bioactive sesterterpene and antiplasmodial alkaloids from the marine sponge *Hyrtios* cf. *erecta*. *J. Nat. Prod.* **2000**, *63* (6), 825-829.
41. Lu, Z.; Ding, Y.; Li, X. C.; Djigbenou, D. R.; Grimberg, B. T.; Ferreira, D.; Ireland, C. M.; Van Wagoner, R. M. 3-bromohomofascaplysin A, a fascaplysin analogue from a Fijian *Didemnum* sp. ascidian. *Bioorg. Med. Chem.* **2011**, *19* (22), 6604-6607.
42. Jimenez, C.; Quinoa, E.; Adamczeski, M.; Hunter, L. M.; Crews, P. Novel sponge-derived amino acids. 12. Tryptophan-derived pigments and accompanying sesterterpenes from *Fascaplysinopsis reticulata*. *J. Org. Chem.* **1991**, *56* (10), 3403-3410.
43. Wildermuth, R.; Speck, K.; Haut, F.-L.; Mayer, P.; Karge, B.; Brönstrup, M.; Magauer, T. A modular synthesis of tetracyclic meroterpenoid antibiotics. *Nat. Commun.* **2017**, *8* (1), 1-9.
44. Kuan, K. K.; Pepper, H. P.; Bloch, W. M.; George, J. H. Total synthesis of (+)-aureol. *Org. Lett.* **2012**, *14* (18), 4710-4713.
45. Sheldrick, G. M. SHELXT - integrated space-group and crystal-structure determination. *Acta Crystallogr. A.* **2015**, *71* (1), 3-8.
46. Dolomanov, O. V.; Bourhis, L. J.; Gildea, R. J.; Howard, J. A.; Puschmann, H. OLEX2: a complete structure solution, refinement and analysis program. *J. Appl. Crystallogr.* **2009**, *42* (2), 339-341.
47. Sheldrick, G. M. Crystal structure refinement with SHELXL. *Acta Crystallogr. C.* **2015**, *71* (1), 3-8.
48. Crystallographic data for compound 11 reported in this paper have been deposited with the Cambridge Crystallographic Data Centre (Deposition number CCDC 2132470). Copies of the data can be obtained, free of charge, on application to the Director, CCDC, 12 Union Road, Cambridge CB2 1EZ, UK (fax: +44-(0)1223-336033 or e-mail: deposit@ccdc.cam.ac.uk)